X-Ray Binaries

56

Jorge Casares, Peter Gustaaf Jonker, and Garik Israelian

Abstract

This chapter discusses the implications of X-ray binaries on our knowledge of Type Ibc and Type II supernovae. X-ray binaries contain accreting neutron stars and stellar-mass black holes which are the end points of massive star evolution. Studying these remnants thus provides clues to understanding the evolutionary processes that lead to their formation. We focus here on the distributions of dynamical masses, space velocities, and chemical anomalies of their companion stars. These three observational features provide unique information on the physics of core collapse and supernovae explosions within interacting binary systems. There is suggestive evidence for a gap between $\approx$2 and 5 $M_{\odot}$ in the observed mass distribution. This might be related to the physics of the supernova explosions although selections effects and possible systematics may be important. The difference between neutron star mass measurements in low-mass X-ray binaries (LMXBs) and pulsar masses in high-mass X-ray binaries

J. Casares (✉)
Instituto de Astrofísica de Canarias, La Laguna, Tenerife, Spain

Departamento de Astrofísica, Universidad de La Laguna, La Laguna, Tenerife, Spain

Department of Physics, Astrophysics, University of Oxford, Oxford, UK
e-mail: jorge.casares@iac.es

P.G. Jonker
SRON, Netherlands Institute for Space Research, Utrecht, The Netherlands

Department of Astrophysics/IMAPP, Radboud University Nijmegen, Nijmegen, The Netherlands
e-mail: P.Jonker@sron.nl

G. Israelian
Instituto de Astrofísica de Canarias, La Laguna, Tenerife, Spain

Departamento de Astrofísica, Universidad de La Laguna, La Laguna, Tenerife, Spain
e-mail: gil@iac.es

A.W. Alsabti, P. Murdin (eds.), *Handbook of Supernovae*,
https://doi.org/10.1007/978-3-319-21846-5_111

(HMXBs) reflects their different accretion histories, with the latter presenting values close to birth masses. On the other hand, black holes in LMXBs appear to be limited to $\lesssim 12\,M_\odot$ because of strong mass loss during the wind Wolf-Rayet phase. Detailed studies of a limited sample of black hole X-ray binaries suggest that the more massive black holes have a lower space velocity, which could be explained if they formed through direct collapse. Conversely, the formation of low-mass black holes through a supernova explosion implies that large escape velocities are possible through ensuing natal and/or Blaauw kicks. Finally, chemical abundance studies of the companion stars in seven X-ray binaries indicate they are metal rich (all except GRO J1655-40) and possess large peculiar abundances of α-elements. Comparison with supernova models is, however, not straightforward given current uncertainties in model parameters such as mixing.

Contents

1 Introduction

X-ray binaries contain compact stellar remnants accreting from "normal" companion stars. Therefore, they provide ideal opportunities for probing the core collapse of massive stars in a binary environment and are thus able to constrain the physics of Type Ibc and Type II supernovae. These compact remnants are revealed by persistent/transient X-ray activity which is triggered by mass accretion. Observationally, they come in three flavors – pulsars, neutron stars, and black holes – that are paired with companion (donor) stars of a wide range of masses. Historically, X-ray binaries have been classified according to the donor mass as either low-mass X-ray binaries (LMXBs) or high-mass X-ray binaries (HMXBs). The former are fueled by accretion disks supplied by a $\lesssim 1\,M_\odot$ Roche-lobe filling star, while HMXBs are mostly fed directly from the winds of a $\gtrsim 10\,M_\odot$ companion. They display distinct Galactic distributions associated with Population I and Population II objects, with

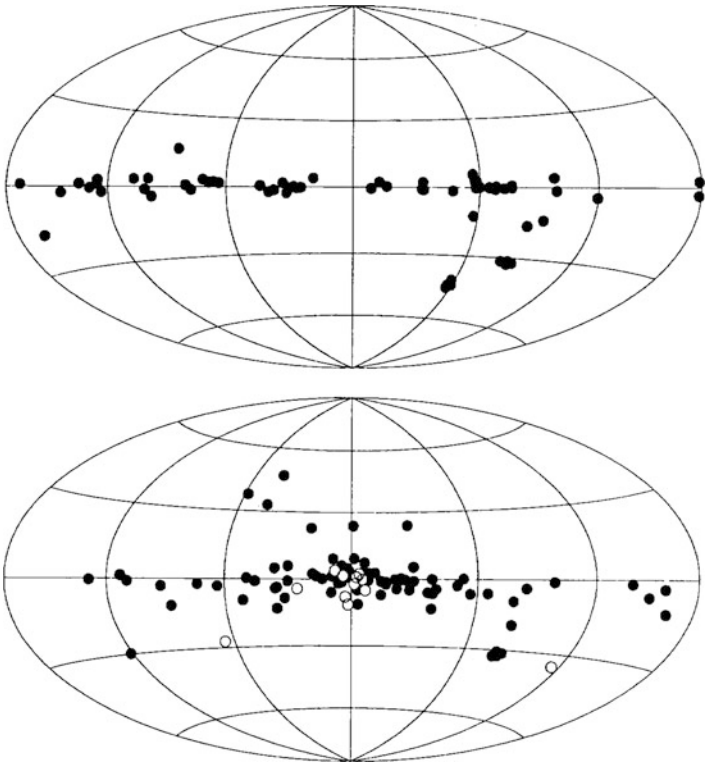

Fig. 1 Galactic distribution of HMXBs (*top*) and LMXBs (*bottom*). *Open circles* indicate LMXBs in globular clusters (From van Paradijs 1998)

HMXBs lying along the Galactic plane and LMXBs clustering toward the Galactic bulge and in globular clusters Joss and Rappaport (1984) (Fig. 1). A handful of X-ray binaries with $\approx 1 - 3\,M_{\odot}$ Roche-lobe filling companions are sometimes referred to as intermediate mass X-ray binaries (IMXBs). For a comprehensive review on X-ray binaries, we refer to Charles and Coe (2006).

The type of X-ray activity observed is determined by (i) the mass transfer rate from the donor, (ii) the magnetic field of the compact star, and (iii) the X-ray heating of the accretion disk by the accretion luminosity. The interplay between these three quantities explains why black hole remnants are mostly found in transient LMXBs, neutron stars in persistent LMXBs, and pulsars in HMXBs. In recent years we have seen the discovery of pulsars with millisecond spin periods in transient LMXBs. These are considered a missing link in X-ray binary evolution, with neutron stars being spun up by sustained accretion to become *recycled* pulsars (Alpar et al. 1982; Wijnands and van der Klis 1998). A detailed review of X-ray binary evolution with the variety of evolutionary paths and end products can be found in ▸ Chap. 57, "Supernovae and the Evolution of Close Binary Systems" (see paragraph "Cross-References").

X-ray binaries present ideal laboratories for examining the physics of the supernova explosions which formed their compact objects. The orbital motion of the stellar companions can be used to weigh the masses of the supernova remnants. Abundance anomalies are often seen in the companion star atmospheres, demonstrating chemical pollution by the supernova ejecta. And the spatial motion of the binary possesses information on the kick velocity imparted by the explosion itself. These three topics (dynamical masses, kick velocities, and chemical anomalies) and their impact on our understanding of Type Ibc and Type II supernovae are the scope of this chapter and will be presented in turn.

2 Remnant Masses

The distribution of masses of compact remnants contains the imprints of the physics of the supernova explosions. Various aspects, such as the explosion energy, mass cut, amount of fallback, or the explosion mechanism itself, are important for the final remnant mass distribution. By building the mass spectrum of compact objects in X-ray binaries, we can therefore obtain new insights onto the physics of core collapse in Type Ibc and Type II supernovae. In principle, precise masses can be extracted from eclipsing double-line spectroscopic binaries using simple geometry and Kepler's laws, but this is not often the case in X-ray binaries. Note that neutron star masses in binary radio pulsars are not discussed here (see ▶ Chap. 47, "The Masses of Neutron Stars"). It should also be noted that the accretion process responsible for lighting up the X-ray binaries can in principle change significantly the neutron star mass in systems where sufficient time is available such as neutron stars in old LMXBs. On the other hand, the accreted mass is too low to alter the BH mass significantly and similarly; the neutron star mass in short-lived HMXBs can also not be changed significantly.

2.1 Pulsar Masses in HMXBs

Pulsars in eclipsing binaries present, in principle, the best prospects for accurate determination of remnant masses. The Doppler shift of the donor's photospheric lines, combined with timing delays of the neutron star pulse, allows us to measure the projected orbital velocities of the two binary components ($K_{\rm opt}$ and $K_{\rm X}$, respectively), thus making them double-lined binaries. If the pulsar is eclipsed by the massive donor (a $\approx 40\,\%$ chance in incipient Roche-lobe overflowing systems), then the inclination angle i is given by

$$\sin i = \frac{\sqrt{1-(R_{\rm opt}/a)^2}}{\cos\theta} \tag{1}$$

where θ is the eclipse half-angle, a the binary separation, and $R_{\rm opt}$ the stellar radius. The latter can be approximated by some fraction $\beta \leq 1$ of the effective Roche-lobe radius $R_{\rm Lopt}$, also known as the stellar "filling factor," while $R_{\rm Lopt}/a$ is purely

a function of the binary mass ratio $Q = M_X/M_{opt} = K_{opt}/K_X$ and the degree of stellar synchronization Ω (usually $\Omega \approx 1$). The stellar masses can then be solved from the mass function equations

$$M_{opt} = \frac{K_X^3 P(1-e^2)^{3/2}}{2\pi G \sin^3 i}(1+Q)^2 \tag{2}$$

$$M_X = \frac{K_{opt}^3 P(1-e^2)^{3/2}}{2\pi G \sin^3 i}\left(1+\frac{1}{Q}\right)^2 \tag{3}$$

where P stands for the binary period and e the orbital eccentricity. This method has produced nine pulsar masses with relatively high precision which we list in Table 1. The major source of uncertainty arises from the combined effect of variable stellar wind, tidal pulsations, and X-ray irradiation which distort the absorption profiles and hence the radial velocity curve of the optical companion (e.g., Quaintrell et al. 2003 and Reynolds et al. 1997). Although not a pulsar, we have also included in this section a remnant mass determination for the eclipsing HMXB 4U 1700-37. With a mass significantly higher than the nine HMXB pulsars, the nature of the compact object in this system is unclear, and a low-mass black hole cannot be dismissed. In any case, the quoted mass should be regarded as somewhat less secure because it rests upon the spectroscopic mass of the optical companion (see Clark et al. 2002 for details).

Interestingly, the largest known population of pulsar X-ray binaries (over 100) belongs to the subclass of Be/X-ray binaries (Reig 2011). These systems generally have very wide and eccentric orbits, with the neutron star accreting material from the circumstellar Be disk during periastron passages or through episodic disk instability events. Unfortunately, the scarcity of eclipsing systems and the very long orbital periods make reliable mass determination in Be/X-ray binaries extremely difficult.

2.2 Neutron Star Masses in LMXBs

Neutron stars in LMXBs do not usually pulse (with 4U 1822-371 and a handful of millisecond pulsars as the only exceptions), and their radial velocity curves are thus not available. Only the mass function of the compact star is attainable through the radial velocity curve of the optical companion (Eq. 3). In these cases it is still possible to derive reliable masses by exploiting the fact that the low-mass donor star overflows its Roche lobe and is synchronized in a circular orbit (which in turn implies $\Omega = 1, e = 1$). This is a reasonable assumption given the long lifetimes and short circularization timescales expected in LMXBs (Witte and Savonije 2001). On this basis, the broadening of the donor absorption lines $V \sin i$ depends on binary mass ratio $q = Q^{-1}$ according to Wade and Horne (1988)

$$V \sin i / K_{opt} \simeq 0.462\, q^{(1/3)}(1+q)^{(2/3)} \tag{4}$$

while its orbital light curve (governed by tidal distortions) correlates with inclination. Therefore, the detection of the faint donor star in LMXBs ensures a full

dynamical solution which makes this technique feasible for transient LMXBs in quiescence (i.e., when accretion is halted and X-ray emission is weak) or persistent LMXBs with long orbital periods and thus luminous companion stars.

In the case of persistent LMXBs with short periods $\lesssim$1 d, the companion star is totally overwhelmed by the accretion luminosity. However, some constraints on stellar masses can still be derived through the Bowen technique which employs fluorescence lines excited on the X-ray heated face of the donor star (Steeghs and Casares 2002). The radial velocity curves of the Bowen lines are biased because they arise from the irradiated face of the star instead of its center of mass. Therefore, a *K-correction* needs to be applied in order to recover the true velocity semi-amplitude $K_{\rm opt}$. The *K-correction* parametrizes the displacement of the center of light with respect to the donor's center of mass through the mass ratio and disk flaring angle α, with the latter dictating the size of the disk shadow projected over the irradiated donor (Muñoz-Darias et al. 2005). Extra information on q and α is thus required to measure the real $K_{\rm opt}$. Further limits to neutron star masses can be set if the binary inclination is well constrained through eclipses (e.g., 4U 1822-371). It is interesting to note that the Bowen technique, despite its limitations, has enabled the first dynamical constraints in persistent LMXBs since their discovery 50 years ago. The best neutron star masses in LMXBs obtained by means of these techniques are also listed in Table 1.

Table 1 Pulsar and neutron star (NS) masses in X-ray binaries[a]

Object	X-ray binary class	Remnant	Mass ($M_\odot$)	References
OAO 1657-415	HMXB/persistent	X-ray pulsar	1.42±0.26	Mason et al. (2012)
SAX 18027-2016	„	„	1.2-1.9	Mason et al. (2011b)
EXO 1722-363	„	„	1.55±0.45	Mason et al. (2011a)
4U 1538-52	„	„	1.00±0.10	
SMC X-1	„	„	1.04±0.09	
Vel X-1	„	„	1.77±0.08	
LMC X-4	„	„	1.29±0.05	
Cen X-3	„	„	1.49±0.08	
4U 1700-37	„	?	2.44±0.27	Clark et al. (2002)
Her X-1	IMXB/persistent	X-ray pulsar	1.07±0.36	
Cyg X-2	LMXB/persistent	NS	1.71±0.21	Casares et al. (2010)
V395 Car	„	„	1.44±0.10	
Sco X-1	„	„	<1.73	Mata Sánchez et al. (2015)
XTE J2123-058	LMXB/transient	„	$1.46^{+0.30}_{-0.39}$	Tomsick et al. (2002)
Cen X-4	„	„	$1.94^{+0.37}_{-0.85}$	Shahbaz et al. (2014)
4U 1822-371	„	X-ray pulsar	1.52-1.85	Muñoz-Darias et al. (2008)
XTE J1814-338	„	msec „	$2.0^{+0.7}_{-0.5}$	Wang et al. (2017)
SAX J1808.4-3658	„	„ „	<1.4	
HETE 1900.1-2455	„	„ „	<2.4	

[a] Adopted from Zhang et al. (2011) and Rawls et al. (2011), unless otherwise stated in the reference column

2.3 Black Hole Masses

The great majority of accreting black holes are found in transient LMXBs/IMXBs, as proved by dynamical studies. Relatively precise masses have been measured in quiescence through exploiting the photometric and spectroscopic detection of the companion star. These are listed in Table 2. Only in the case of GX 339-4 is the constraint on the black hole mass aided by the Bowen technique. In some cases uncertainties are quite large owing to possible systematics affecting the determination of the binary inclination angle. In others, only a robust lower limit to the black hole mass is secured by the spectroscopic mass function combined with the absence of X-ray eclipses.

Five additional black holes have now been established in HMXBs. Although the companion star underfills its Roche lobe in these systems, extra information on the stellar radius is granted by very precise distance determinations ($\lesssim$5 % e.g., through

Table 2 Black hole masses in X-ray binaries[a]

Object	X-ray binary class	Mass ($M_\odot$)	References
GRS 1915+105	LMXB/transient	$12.4^{+2.0}_{-1.8}$	Reid et al. (2014)
V404 Cyg	„	$9.0^{+0.2}_{-0.6}$	
BW Cir	„	>7.0	
GX 339-4	„	>6.0	
XTE J1550-564	„	7.8−15.6	
H1705-250	„	4.9−7.9	
GS 1124-684	„	$11.0^{+2.1}_{-1.4}$	Wu et al. (2016)
GS 2000+250	„	5.5−8.8	
A0620-00	„	6.6±0.3	
XTE J1650-500	„	4.0−7.3	
GRS 1009-45	„	>3.6	
XTE J1859+226	„	>5.42	
GRO J0422+32	„	>1.6	
XTE J1118+480	„	6.9−8.2	
XTE J1819.3-2525	IMXB/transient	6.4±0.6	Macdonald et al. (2014)
GRO J1655-40	„	5.4±0.3	
4U 1543-475	„	2.7−7.5	
Cyg X-1	HMXB/persistent	14.8±1.0	
LMC X-1	„	10.9±1.4	
LMC X-3	„	7.0±0.6	Orosz et al. (2014)
M33 X-7	„	15.7±1.5	
MWC 656	HMXB/transient (?)	3.8−5.6	Casares et al. (2014)

[a]Adopted from Casares and Jonker (2014) unless otherwise stated in the reference column. Lower limits for BW Cir, GRS 1009-45, XTE J1859 + 226, and GRO J0422 + 32 are based on the absence of eclipses, combined with updated determinations of the mass function and q (when available). The lower limit on GX 339-4 is based on the lack of X-ray eclipses plus constraints provided by the *K-correction*

VLBI parallax for Cyg X-1) coupled with the observed apparent brightness and effective temperature. Furthermore, in the case of M33 X-7, eclipses of the X-ray source by the donor star provide additional tight constraints on the inclination which results in one of the largest accurately known black hole masses.

Note that we have excluded mass measurements for the two extragalactic HMXBs NGC 300 X-1 and IC 10 X-1. This is because these rely on radial velocity curves of the HeII λ4686 wind emission line and an assumed mass for the Wolf-Rayet star. Different groups have reported conflicting results which range from canonical neutron stars to the largest black hole masses measured so far and are hence unreliable. The table includes MWC 656, the first black hole companion to a Be star (Casares et al. 2014). Here the black hole mass relies on the spectroscopic mass of the optical companion and the radial velocity curves of the two stars, extracted from the dynamics of circumstellar gaseous disks. A critical review of black hole mass determinations, including potential systematic effects, is presented in Casares and Jonker (2014).

2.4 The Mass Spectrum: Implications for Supernovae Models

Figure 2 presents the observed masses of neutron star and black hole remnants in X-ray binaries, as in Tables 1 and 2. Note that we have here excluded neutron star masses in radio pulsars and binary millisecond pulsars (as discussed in ▸ Chap. 47, "The Masses of Neutron Stars"). The bottom panel displays the number distributions of neutron stars (black) and black holes (red) masses, excluding upper/lower limits. Three main features seem to be drawn from the plot, namely, (1) neutron star masses tend to be larger in LMXBs/IMXBs (mass average of $1.54 \pm 0.16\,M_\odot$) than in HMXBs ($1.34 \pm 0.26\,M_\odot$), (2) a dearth of remnants or gap appears between $\sim$2 and $5\,M_\odot$, and (3) the most massive black holes ($\sim 15\,M_\odot$) are found in HMXBs.

Feature (1), although tentative, could be a manifestation of the pulsar recycling scenario. The difference in neutron star masses, if confirmed, would stem from different binary evolution histories, with neutron stars in LMXBs having experienced significant accretion over extended periods of time. This interpretation would be further supported by indications that pulsar mass decreases with spin period (Zhang et al. 2011). Neutron stars in HMXBs are little modified by accretion, and, thus, their masses are expected to lie closer to their birth values. And indeed, both the mean and dispersion of the neutron star mass distribution in HMXBs are found to agree with theoretical expectations of core-collapse supernovae (Özel, et al. 2012). Constraints on neutron star forming supernovae do seem to be provided by two distinct populations of X-ray pulsars in Be/X-ray binaries; short $P_{\rm spin}$ pulsars with short orbital periods and low eccentricities would be produced by electron-capture supernovae, while long $P_{\rm spin}$ pulsars with long orbital periods and high eccentricities in iron-core-collapse supernovae (Knigge et al. 2011). The former pulsars are naturally expected to be less massive ($\lesssim 1.3\,M_\odot$), but, unfortunately, this cannot yet be tested because of the lack of precise neutron star mass determinations in Be/X-ray binaries.

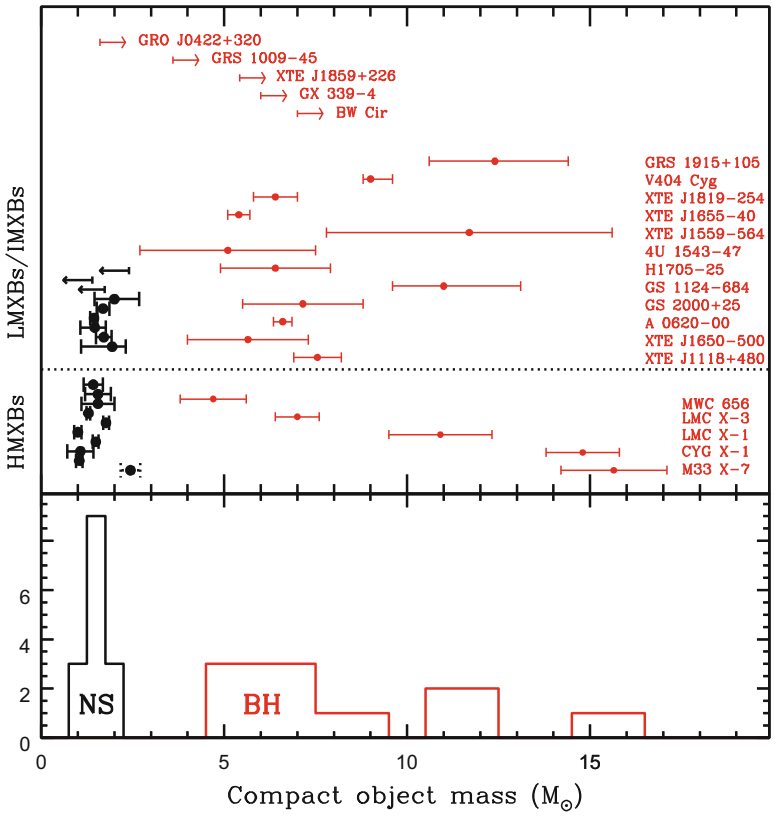

Fig. 2 *Top*: compact remnant masses measured in X-ray binaries. Neutron stars and black holes are indicated in *black* and *red colors*, respectively. 4U 1700-37 is plotted in *dotted-style line* because the nature of the compact star is uncertain. The *horizontal dotted line* divides LXMBs/IMXBs from HMXBs. *Bottom*: observed distribution of neutron stars and black hole masses

Feature (2) is a statistically robust property of the mass spectrum (see Farr et al. 2011 and references therein). The lack of compact remnants between $\sim$2 and 5 $M_\odot$ contrasts with numerical simulations of supernova explosions by Fryer and Kalogera (2001) that lead to continuous distributions and typical exponential decays. These simulations, however, are based on single star populations with a heuristic treatment of binarity through Wolf-Rayet winds following common envelope evolution. In order to accommodate the evidence of a mass gap, a discontinuous dependence of explosion energy with progenitor mass seems unavoidable. In this context, it has been proposed that convection (Rayleigh-Taylor) instabilities, growing within 200 ms after core bounce, can successfully revive the supernova shock and trigger the explosion, thereby causing the gap (see Fig. 3, but also Ugliano et al. 2012 for a different interpretation based on neutrino-driven explosion models).

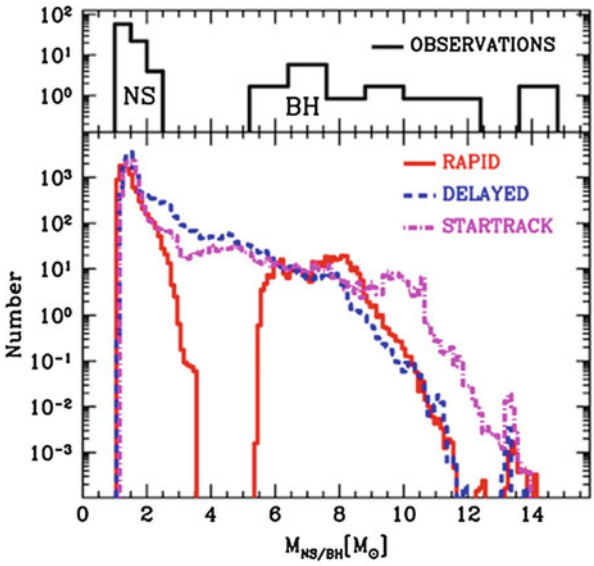

Fig. 3 Observed mass distribution of compact objects in X-ray binaries (*top*), compared to theoretical distributions computed for different supernova models (*bottom*). The mass gap can be reproduced only if turbulent instabilities grow rapidly. Slow growing instabilities lead to significant fallback that would fill the mass gap (From Belczynski et al. 2012)

Alternatively, a gap can be produced if red supergiant stars of $\approx$17–25 $M_\odot$ suffer a failed supernova explosion, leaving a remnant with the mass of the He core while ejecting the weakly bound H envelope (Kochanek 2014). This interpretation appears attractive because in turn it provides an explanation for the deficit of high-mass progenitors seen in pre-explosion images of Type IIp supernovae (Smartt et al. 2009). On the other hand, it fails to account for the peculiar abundance of α-elements detected in the companion stars which demands significant contamination from supernova ejecta (see Sect. 4). It is also unclear how very wide binaries with such red supergiants can evolve to form the compact black hole binaries that we see today.

Feature (3) most likely reflects different binary evolutionary paths, with black holes in LMXBs being limited to $\lesssim$12 $M_\odot$ by severe mass loss from the Wolf-Rayet progenitor after the common envelope phase (Fryer and Kalogera 2001). Conversely, black holes in HMXBs can grow from more massive stars, especially in low-metallicity environments such as in the case of M33 X-7. Furthermore, it is possible that the progenitor star evolves through the He burning phase still embedded in the H envelope (case C mass transfer), thus suffering less wind mass loss (Brown et al. 2001). However, it should be noted that some aspects of binary and massive stellar evolution (e.g., radial expansion, wind mass loss rates, efficiency of common envelope ejection) are still quite uncertain, which certainly limits our understanding of the formation of X-ray binaries.

At this point, the impact of systematic uncertainties in the determination of binary inclination angles should also be stressed, as exemplified by the large dispersion of values reported by independent groups on individual systems (see Casares and Jonker 2014). Ignoring the role of systematics can lead to overestimated black hole

masses and hence a bias in the observed distribution (Kreidberg et al. 2012). In addition, the sample of X-ray binaries with dynamical mass determinations is almost certainly prone to complex selection effects (both evolutionary and observational) not completely understood. For instance, it may be possible that low-mass black holes become unbound by the supernova explosion or are hidden in very faint (but persistent) X-ray binaries. The system MWC 656 might be itself a member of a hidden population of very faint low-mass black holes. More observational work is required to enlarge the sample of secure black hole masses before the observed distribution can be definitively used to illuminate the properties of the supernova engine.

3 Kick Velocities

For this section we focus on stellar-mass black holes in X-ray binaries rather than neutron star X-ray binary systems as their space velocities are more readily measured using pulsar timing information (González et al. 2011). Both the black hole mass and its spin as well as the black hole's velocity through space are almost exclusively set at the instant of formation. The black hole spin and mass do not change appreciably during its subsequent evolution. Even the accretion of material that allows us to discover these sources as black hole X-ray binaries when they outburst does not change these parameters. The reason is that in order to affect the black hole spin or mass significantly, one needs to accrete of order the black hole mass. Due to the Eddington limit and the limited amount of mass available from a stellar-mass donor star, this is not possible. Encounters with giant molecular clouds and spiral density waves result in changes in the gravitational potential (Wielen 1977), and these *can* change the space velocity of stellar-mass black holes in X-ray binaries as they travel through our Galaxy in the Gyrs after their formation. The magnitude of velocity changes depends on the age of the system and can at most amount up to $40\,\mathrm{km\,s^{-1}}$ as determined for late-type (single) stars from Hipparcos data by Dehnen and Binney (1998). Thus, with the caveat on space velocities less than $\sim 40\,\mathrm{km\,s^{-1}}$, these parameters are a prior for the black hole formation mechanism, providing input on the black hole formation and supernova models.

3.1 Black Hole Formation and Its Link to Space Velocity

Models for black hole formation distinguish two formation scenarios (Fryer and Kalogera 2001): either direct or delayed collapse where in the latter a neutron star is formed first which moments later collapses into a black hole. The more massive progenitor stars could collapse directly to a black hole without producing a strong supernova. The latter scenario is in line with the absence of supernovae from red supergiants more massive than $\sim 18-20\,\mathrm{M}_\odot$ (Smartt 2015). Instead of a supernova, the event marking the birth of a black hole could be a faint, short-duration (3–10 days) blue transient that may form from direct collapse red supergiant progenitors

as the shock caused by the response of the stellar envelope to neutrino emission in the collapsing core equivalent to a few times $0.1\,M_\odot$ of rest mass energy breaks out of the star (Piro 2013). Others propose that also a red transient with a longer time scale will ensue, which should be of the order of a year (Lovegrove and Woosley 2013; O'Connor and Ott 2011). Candidate failed supernovae of a red supergiant have been reported: one in NGC 6946 (Gerke et al. 2015) and one in NGC 3021 (Reynolds et al. 2015). Given the brightness of red supergiants in the near-infrared, a dedicated near-infrared variability study of nearby galaxies could have a good chance of finding such events, even though some Mira and R Coronae Borealis variables may have similar characteristics (although in the failed supernova and black hole formation case, the transient should fade away indefinitely).

The main uncertainties in the theoretical supernova and (binary) massive star evolution calculations stem from uncertainties in the supernova explosion mechanism for stars with progenitor masses in the range between 11 and approximately $30\,M_\odot$ and also from uncertainties in the amount of mass lost during the evolution for stars with progenitor masses above approximately $30\,M_\odot$. Neutrino-driven supernova models (e.g., Ugliano et al. 2012) seem compatible with the observed black hole mass distribution reported in Özel et al. (2010) and Farr et al. (2011) with an apparent lack of low-mass black holes in the mass range of $2–5\,M_\odot$ (see Sect. 2).

The direct collapse and the delayed proto-neutron star collapse models might be responsible for the formation of different mass black holes, and also different space velocities. Direct collapse produces a black hole without much of a kick, whereas the delayed supernova models produce relatively low-mass black holes that receive a larger kick and thus space velocity.

3.2 The Black Hole Space Velocity

The difference between the velocity of a (black hole) system and that expected for its local standard of rest is called the space velocity. Occasionally, this velocity is called "peculiar velocity," but this term is also often used to indicate the velocity difference between the Hubble flow and the velocity of galaxies. Hence to avoid confusion, we use "space velocity" for the black hole binary systems.

It has been inferred from the velocity distribution of neutron stars observable as single radio pulsars that they receive a kick at birth due to asymmetries in the supernova explosion (Lyne and Lorimer 1994). This we call a natal kick. Black holes forming from fallback onto a proto-neutron star should then also get such a natal kick, resulting potentially in a significant space velocity. The magnitude would depend on whether the natal kick momentum for a neutron star and proto-neutron star that collapses to a black hole is the same or not. In addition to such a natal kick, in any supernova explosion in a binary where mass is lost from the binary system, a kick should be imparted on the system irrespective of the type of compact object formed during the supernova (Blaauw 1961). The binary will be disrupted if more than half the total binary mass is ejected in the supernova. Therefore, this sets an upper limit to the amplitude of such a so-called Blaauw kick (Nelemans et al.

1999). Information that can help differentiating between a Blaauw and a natal kick is that a Blaauw kick is directed in the binary plane (unless the supernova mass loss is not symmetric), whereas a natal kick may not be restricted to that plane. Given that large natal kick velocities yield a higher probability to unbind the binary system, a population synthesis model explaining the observed black hole X-ray binary mass and space velocity distribution has to be used to correct for this bias (e.g., Belczynski et al. 2012).

Evidence for velocity kicks in neutron star, as well as black hole low-mass X-ray binaries, comes from the fact that they have, on average, a large distance to the plane of the Galaxy (Jonker and Nelemans 2004; Repetto and Nelemans 2015; van Paradijs and White 1995). Evidence for kicks in the formation of LMXBs also comes from their observed distribution in early-type galaxies. The LMXBs extend further than the stellar light consistent with a population of kicked LMXBs (Zhang et al. 2013). In contrast, given that LMXBs are also found in the Large Magellanic Cloud and perhaps dwarf galaxies (cf. Maccarone et al. 2005), a fraction must receive a small kick velocity upon formation; otherwise, they would not be found in those systems given their low escape velocities. Similarly, the recent evidence for the presence of black holes in globular clusters (e.g., Chomiuk et al. 2013; Strader et al. 2012) implies a population of low natal kick black holes.

3.3 Measuring the Space Velocity

For individual sources the space velocity can be determined as follows: the optical or near-infrared spectroscopic observations providing the mass function via the measurement of the radial velocity amplitude (see Sect. 2) will also provide the systemic radial velocity if, in the cross-correlation of the source and template spectra, the template is a radial velocity standard or a model atmosphere. In order to calculate the space velocity of the X-ray binary, its systemic radial velocity has to be combined with a proper motion and distance measurement.

Ideally, as it depends on geometry alone, the distance is measured through a (radio) parallax measurement. However, in practice, parallax measurements have so far only been possible for three black hole X-ray binaries: V404 Cyg (Miller-Jones et al. 2009b), Cyg X-1 (Reid et al. 2011), and GRS 1915+105 (Reid et al. 2014). The main reasons why a parallax measurement has been possible for these three systems is that V404 Cyg is bright in quiescence when compared to the other systems (cf. Miller-Jones et al. 2011), and the latter two black holes are virtually always actively accreting matter, which makes that the time baseline necessary for a parallax measurement is long enough. However, while always accreting, the last two sources are not always in the accretion state that allows a compact radio jet to be formed, which still made the detection of the parallax signal difficult (see the discussion in Reid et al. 2014). For the vast majority of black hole X-ray transients, a parallax measurement has not been possible. A major obstacle in the measurements has been the short duration of outbursts. The month-long outburst coupled with the aforementioned state changes does not allow for the measurements

necessary to detect the often small parallax signals. The best future hope for parallax signal detection comes from a few sources that show recurrent outbursts such as GX 339–4.

The second-best distance determination comes from what is often called a photometric parallax. Here, one compares the apparent magnitude of the companion (= mass donor) star with its absolute magnitude to determine the distance. However, the effect of interstellar extinction influences the apparent magnitude, it causes the star to appear fainter and redder, and hence one would put it further away than it really is if these effects are not corrected for. Furthermore, more often than not, residual light is produced by the accretion disk, making the system appear brighter. The disk contribution can be determined from optical spectroscopic observations, but it is not constant in time (Cantrell et al. 2008), complicating the determination of the correction factor. The fact that the star is losing mass influences the radius of the star, and as such it is not the same as that of a single star of the same spectral type and luminosity class. Hence, its radius has to be determined from the data. Finally, in accreting black hole X-ray binary systems such as under consideration here, the star is very likely to be in forced corotation with the orbit making it rotate around its axis fast which may influence the absolute magnitude of the star. Studies of rapidly rotating early-type stars found that fast rotation causes an increase in absolute magnitude of stars with spectral type later than B5 (the stars are intrinsically less luminous than the nonrotating stars of the same spectral type by typically several tenths of a magnitude (Collins and Sonneborn 1977)).

Additionally, it is known that limb and gravity darkening effects change the equivalent widths of photospheric stellar absorption lines (e.g., Shajn and Struve 1929 and Collins and Sonneborn 1977), which could lead to a slightly erroneous spectral type being obtained from the data. Generally, the lines in the spectrum resemble the lines of a later spectral type. Furthermore, the limb and gravity darkening is different in the distorted Roche-lobe filling mass donor stars compared to single stars. Overall, distances determined via a photometric parallax can easily be off by several tens of percent. See Jonker and Nelemans (2004) for further discussion on these issues.

In contrast with the parallax signal, the accuracy with which proper motions can be detected is higher as the proper motion signal adds over time. The proper motion has been measured using radio very long baseline interferometry (VLBI) of eight black hole X-ray binaries (see Table 3). Recent measurements show the proper motion of the recurrent transient black hole GX 339–4 (Miller-Jones et al. in prep., see Fig. 4). For this source we still need to determine the spectral type of the mass donor star and the accretion disk contribution to the total light in quiescence in order to estimate the distance to the system more accurately using a photometric parallax than what is currently possible (Hynes et al. 2004).

In some cases the location on the sky together with a proper motion measurement can already put strong constraints on the presence of natal kicks. For instance, for the black hole candidate (candidate as no mass measurement for the source exists currently), MAXI J1836-194, evidence from the radio proper motion alone suggests that the source received a kick at birth (see Fig. 5).

Table 3 Proper motions of black hole X-ray binaries

Source name	$\mu_\alpha \cos\delta$ (mas yr^{-1})	μ_δ mas yr^{-1}	References
XTE J1118+480	−16.8±1.6	−7.4±1.6	Mirabel et al. (2001)
GRO J1655–40	−3.3±0.5	−4.0±0.4	Mirabel et al. (2002)
GX 339–4	−3.95±0.07	−4.71±0.06	[a]
Swift J1753.5–0127	1.5±0.4	−3.0±0.4	[a]
MAXI J1836-194	−2.3±0.6	−6.1±1.0	Russell et al. (2015)
GRS 1915+105	−2.86±0.07	−6.20±0.09	Dhawan et al. (2007)
Cyg X-1	−3.78±0.06	−6.40±0.12	Reid et al. (2014)
V404 Cyg	−5.04±0.22	−7.64±0.03	Miller-Jones et al. (2009b)

[a]Miller–Jones et al. in prep

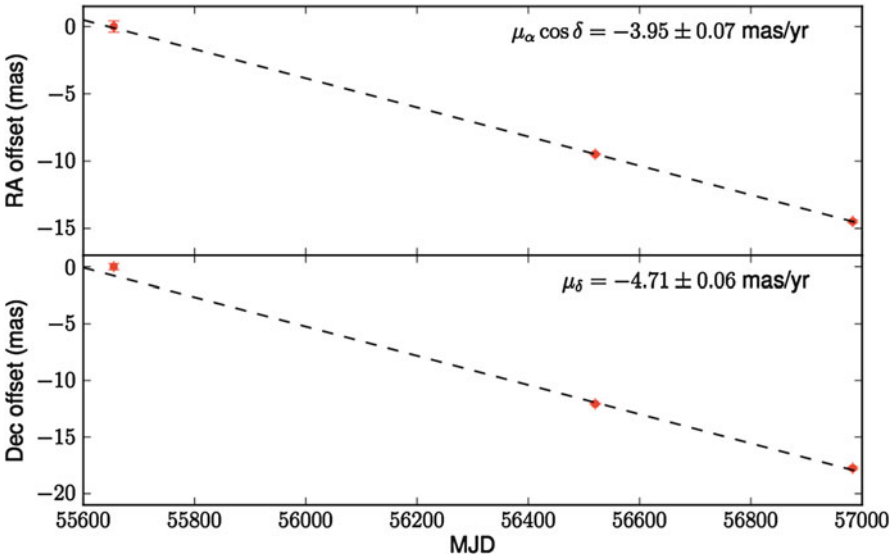

Fig. 4 The proper motion fit to long baseline array radio observations of GX 339-4. Whereas the data is sparse, mostly due to the outburst duty cycle of this source, the proper motion signal is significantly detected (Figure courtesy James Miller–Jones; Miller–Jones et al. in prep.)

Whereas so far all these proper motion measurements have come from radio VLBI measurements, in the near future, the Gaia satellite may also provide proper motion measurements of X-ray binaries. Gaia has been launched in December 19, 2013, and scans the whole sky (including the Galactic plane) at high spatial resolution with accurate photometry down to G = 20.3 and tens of micro-arcsecond astrometry. Gaia consists of two telescopes aligned in a plane with an angle of 106.5° in between. As Gaia scans the sky, it will make many visits of the same region. For most of the sky, the number of visits is ≈70 over a 5-year mission lifetime (and an extension of the mission is possible improving primarily the proper motion measurements). The multiple visits of the same parts of the sky will allow

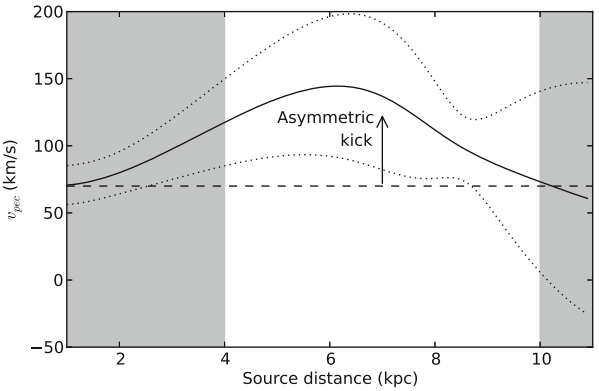

Fig. 5 The asymmetric natal kick exerted on the *black hole* upon formation on *top* of the maximum Blaauw kick possible without disrupting the binary (*dashed line*; Nelemans et al. 1999) required to explain the observed proper motion for the black hole candidate source MAXI J1836–194 (Russell et al. 2015). The *dotted lines* indicate the measurement uncertainties, and the *white area* is the range in distances that is allowed for this particular source. The observables that still need to be measured to determine the space velocity are the systemic radial velocity and the source distance. A model for the Galactic rotation is used (Honma et al. 2012)

the detection of proper motion and parallax signals if the sources are bright enough. Gaia's G-band is effectively a white light band where the bandpass is set by the efficiency of the telescope + CCD.

Proper motion and parallax measurements of several of the black hole X-ray binaries mentioned in Table 3 will be improved. In addition these parameters will be measured for a few sources for which these measurements do not exist currently. An example of the latter is 1A 0620-00. However, the intrinsic and apparent faintness of the often low-mass donor stars is a limiting factor for Gaia's contribution to this field. Many of the black hole X-ray binaries reside in the plane of the Galaxy and are further away than a few kpc, making reddening significant. The fact that they reside in the plane probably hints at a low space velocity as sources spend most of the time at the extremes of their Galactic orbit. In general (non-Gaia) astrometric measurements in the optical or near-infrared are difficult. An obstacle to the required astrometric accuracy is the need to find astrometric "anchors" that tie the frame to the International Celestial Reference System. Background quasars and active galactic nuclei are good candidate anchors, but in the plane their apparent magnitude is reduced also due to the reddening.

Once the position on the sky, the systemic radial velocity, the proper motion, and the distance to the source are known, one can derive the space velocity using the transformations of Johnson and Soderblom (1987) to calculate Galactic velocities in the heliocentric frame, which can then be corrected for the space velocity of the Sun with respect to the local standard of rest ($U = 10.0 \pm 0.36\,km\,s^{-1}$, $V = 5.25 \pm 0.62\,km\,s^{-1}$, $W = 7.17 \pm 0.38\,km\,s^{-1}$; Dehnen and Binney 1998). Here, U is defined as positive toward the Galactic Center, V positive toward $l = 90°$, and W positive toward the north Galactic pole.

3.4 Black Hole X-Ray Binaries with and Without Natal Kicks

Having described in some detail how to measure the parameters that are necessary to determine the space velocity of stellar-mass black holes in X-ray binaries, we now turn to the measured space velocities. The space velocities have been determined for five black hole X-ray binaries only so far. A recent overview of black hole space velocities is presented in Miller-Jones (2014) (his table 2).

Repetto and Nelemans (2015) investigated whether there is evidence for the presence of a natal besides a Blaauw kick taking the binary evolution of seven short orbital period systems into account. The main conclusion is that for at least two systems, a natal kick is necessary. In addition, five systems could be well explained with a natal kick but virtually no ejection of mass in a supernova, such as in direct collapse scenarios.

Natal kicks are probably necessary for the black hole X-ray binaries XTE J1118+480 (Gualandris et al. 2005) and GRO J1655–40 (Willems et al. 2005) and are likely for V404 Cygni (Miller-Jones et al. 2009a). Cygnus X-1 and GRS 1915+105, on the other hand, were found to have been formed with little or no kick (Mirabel and Rodrigues 2003; Reid et al. 2011, 2014). It is interesting to note that the black holes in Cygnus X-1 and GRS 1915+105 are among the most massive stellar-mass black holes known so far in our Galaxy, which could be interpreted as suggestive evidence for a formation difference between the more massive and lighter stellar-mass black holes. For instance, the more massive black holes could form through direct collapse giving rise to no or only very small space velocities as only a limited amount of mass is lost from the system (minimizing the Blaauw kick) and the maximum natal kick impulse imparted on any proto-neutron star due to asymmetric neutrino emission has an upper limit which equals the binding energy of the maximum mass proto-neutron star that can be formed (Janka 2013). The latter thus would imply that the more massive the black hole formed, the smaller the space velocity acquired. However, in a scenario where the more massive black holes form through a supernova (and not a direct collapse) and when the fallback of the slowest parts of the supernova ejecta is asymmetric, one would produce larger natal kicks for more massive black holes (Janka 2013). Space velocity and black hole mass measurements for more black hole X-ray binaries as well as searches of failed supernovae are necessary to distinguish between these scenarios.

4 Chemical Abundance of Companion Stars

It is conceivable that the supernova explosion that created a black hole or a neutron star remnant in X-ray binaries has modified the physical and chemical characteristics of the secondary star. However, uncertainties in the supernova explosion models affect the predictions of the chemical composition of ejecta captured by the companion. Nevertheless, chemical abundance studies of the companion stars in LMXBs may open a new route to constrain supernova models.

Unfortunately, high-quality spectroscopic observations of LMXBs and their analysis is a serious challenge. The rotation, possible spots, and magnetic activity of the companion star, as well as continuum veiling produced by the residual accretion disk, introduce additional uncertainties. In any case, attempts have been made to minimize the most important sources of uncertainties in the calculation of the stellar parameters and chemical abundances. Nova Scorpii 1994 was the first black hole X-ray binary system for which a detailed abundance study has been carried out (Israelian et al. 1999). Striking overabundance of several α-elements (such as O, S, Si) was discovered and interpreted as a result of a pollution by matter ejected by the supernova.

4.1 Observations, Models, and Spectral Synthesis Tools

The chemical analysis of secondary stars in LMXB systems is influenced by three important factors: veiling from the accretion disk, rotational broadening, and signal-to-noise ratio of the spectra. Moderately strong and relatively unblended lines of chemical elements of interest have to be identified in the high-resolution solar flux atlas. Spectral line data from the Vienna Atomic Line Database can be used to compute synthetic spectra for these features employing a grid of local thermodynamic equilibrium (LTE) models of atmospheres provided by Kurucz (1993, private communication). These models are interpolated for given values of effective temperature [$T_{\rm eff}$], surface gravity [log g], and metallicity [Fe/H].

A grid of synthetic spectra is generated for these features in terms of five free parameters, three to characterize the star atmospheric model ([$T_{\rm eff}$], [log g], and [Fe/H]) and two further parameters to take into account the effect of the accretion disk emission in the stellar spectrum. This veiling is defined as the ratio of the accretion disk flux to the stellar continuum flux, $F_{disc}/F_{cont,star}$. It has been considered as a linear function of wavelength and is thus characterized by two parameters: veiling at 4500Å, $f_{4500} = F^{4500}_{disc}/F^{4500}_{sec}$, and the slope, m_0.

Next, the observed spectra are compared with each synthetic spectrum in the grid (between 800.000 and 1.5 million spectra) via a χ^2 minimization procedure that provides the best model fit. A bootstrap Monte Carlo method using 1000 realizations is typically used to define the 1σ confidence regions for the five free parameters. Figure 6 shows the distributions obtained for the source A0620-00.

4.2 Stellar Abundances

Several spectral regions containing the lines of Si, Ca, Al, Ti, and Ni have been analyzed. Although the lines of these elements were usually the main contributor to the features, in some cases, they were blended with Fe. The inaccuracy in the location of the continuum caused by the blends of many weak rotationally broadened stellar lines was one of the main sources of error in the abundance

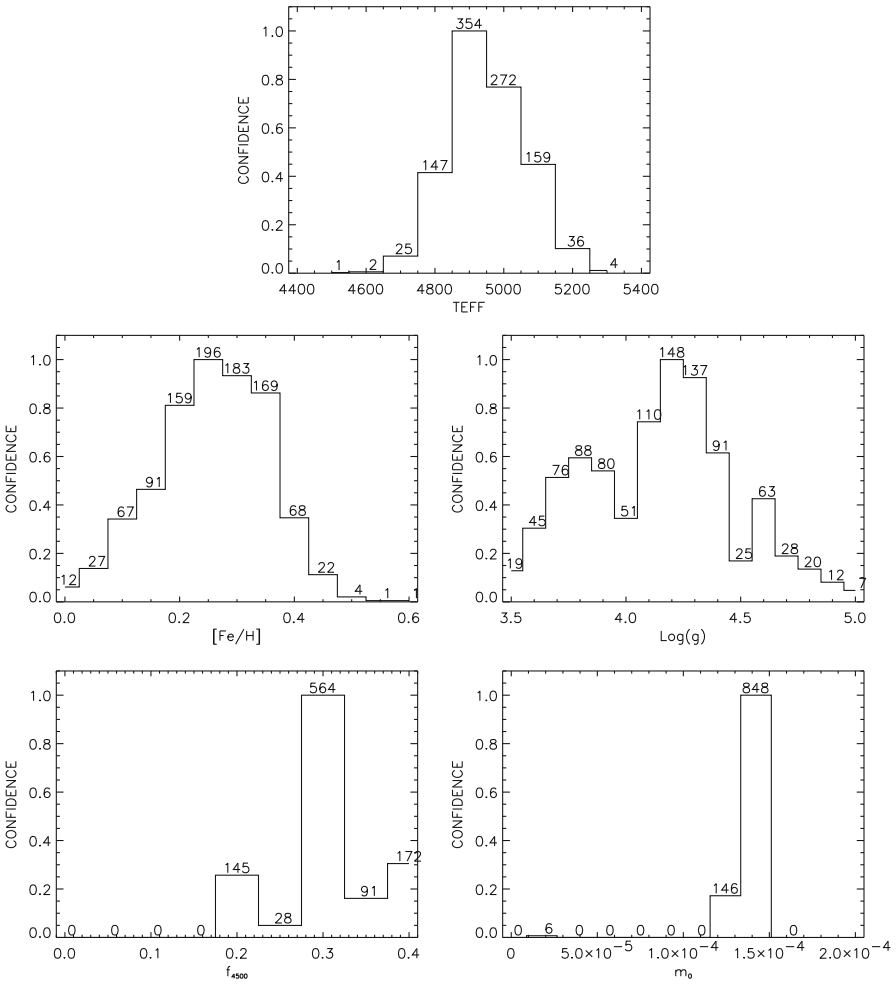

Fig. 6 Distributions obtained for each parameter using Monte Carlo simulations. The labels at the top of each bin indicate the number of simulations consistent with the bin value. The total number of simulations was 1000 (Figure from González Hernández et al. 2004)

determinations. Several examples of the fits to specific absorption lines are shown in Figs. 7 and 8. Most of the results for the LMXB systems studied to date are compiled in Table 4 and reviewed in the next section.

4.3 Individual Systems

4.3.1 Nova Scorpii 1994 (GRO J1655-40)

Keck/HIRES spectrum of this system has been first studied by Israelian et al. (2009, 1999) who discovered that oxygen, sulfur, and silicon are overabundant from eight

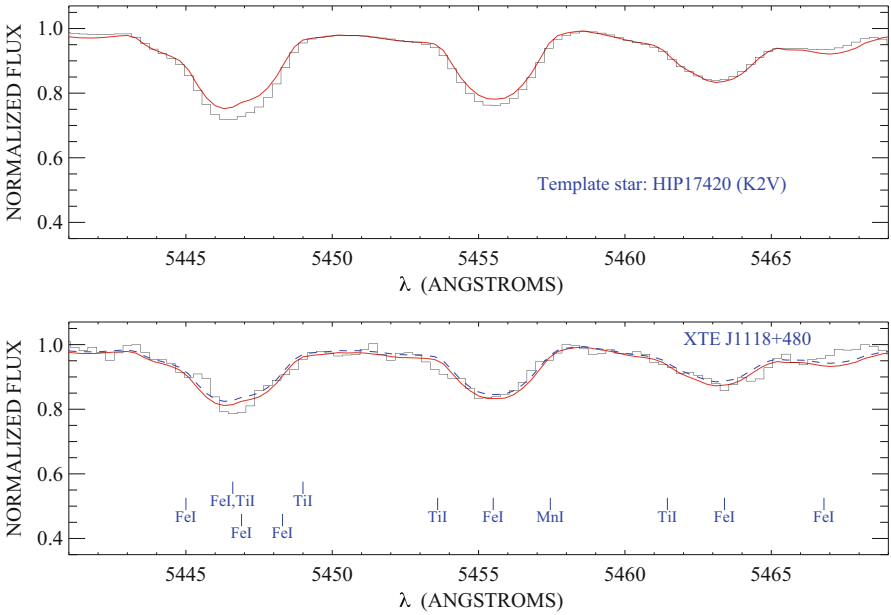

Fig. 7 Best synthetic spectral fits to the Keck/ESI spectrum of the secondary star in the XTE J1118 + 480 system (*bottom panel*) and the same for a template star (properly broadened) shown for comparison (*top panel*). Synthetic spectra are computed for solar abundances (*dashed line*) and best-fit abundances (*solid line*) (This figure is taken from González Hernández et al. 2008b)

to ten times compared to the Sun. The analysis of González Hernández et al. (2008a) based on the VLT/UVES high-resolution spectra confirmed that the abundances of Al, Ca, Ti, Fe, and Ni are consistent with solar values, whereas Na and especially O, Mg, Si, and S are significantly enhanced in comparison with the Sun and Galactic trends of these elements. A comparison with spherically and nonspherically symmetric supernova explosion models may provide stringent constraints to the model parameters as mass cut and the explosion energy, in particular from the relative abundances of Si, S, Ca, Ti, Fe, and Ni.

4.3.2 A 0620-00

It has been shown (González Hernández et al. 2004) that the secondary star in this system is metal rich with [Fe/H] = 0.14 ± 0.20. Nevertheless, the abundances of Fe, Ca, Ti, Al, and Ni are slightly higher than solar. The abundance ratios of each element with respect to Fe were compared with these ratios in late-type main sequence metal-rich stars. Moderate anomalies for Ti, Ni, and especially Al have been found. A comparison with element yields from spherically symmetric supernova explosion models suggests that the secondary star captured part of the ejecta from a supernova that also originated the compact object in A0620-00. The observed abundances can be explained if a progenitor with a 14 $M_{\odot}$ He core

Table 4 Masses, velocity, stellar, veiling parameters, and chemical abundances[a] in LMXBs. See González Hernández et al. (2011) for a definition of the parameters listed in column 1

Star	A0620-00	Centaurus X-4	XTE J1118 + 480	Nova Sco 94	V404 Cygni	Cygnus X-2
Alternative name	V616 Mon	V822 Cen	KV UMa	GRO J1655–40	GS 2023 + 338	V1341 Cyg
$M_{CO,f}$ ($M_\odot$)	6.61 ± 0.25	1.50 ± 0.40	8.30 ± 0.28	6.59 ± 0.45	9.00 ± 0.60	1.71 ± 0.21
$M_{2,f}$ ($M_\odot$)	0.40 ± 0.05	0.30 ± 0.09	0.22 ± 0.07	2.76 ± 0.33	0.54 ± 0.08	0.58 ± 0.23
$v$sini (km s^{-1})	82 ± 2	44 ± 3	100^{+3}_{-11}	86 ± 4	40.8 ± 0.9	34.6 ± 0.1
$T_{\rm eff}$ (K)	4900 ± 100	4500 ± 100	4700 ± 100	6100 ± 200	4800 ± 100	6900 ± 200
$\log(g/{\rm cm\ s^2})$	4.2 ± 0.3	3.9 ± 0.3	4.6 ± 0.3	3.7 ± 0.2	3.50 ± 0.15	2.80 ± 0.20
f_{4500}	0.25 ± 0.05	1.85 ± 0.10	0.85 ± 0.20	0.15 ± 0.05	0.15 ± 0.05	1.55 ± 0.15
$m_0/10^{-4}$	-1.4 ± 0.2	-7.1 ± 0.3	-2 ± 1	-1.2 ± 0.3	-1.3 ± 0.2	-2.7 ± 0.4
[O/H][b]	–	–	–	0.91 ± 0.09	0.60 ± 0.19	0.07 ± 0.35
[Na/H]	–	–	–	0.31 ± 0.26	0.30 ± 0.19	–
[Mg/H]	0.40 ± 0.16	0.35 ± 0.17	0.35 ± 0.25	0.48 ± 0.15	0.00 ± 0.11	0.87 ± 0.24
[Al/H]	0.40 ± 0.12	0.30 ± 0.17	0.60 ± 0.20	0.05 ± 0.18	0.38 ± 0.09	–
[Si/H]	–	–	0.37 ± 0.21	0.58 ± 0.08	0.36 ± 0.11	0.52 ± 0.22
[S/H]	–	–	–	0.66 ± 0.12	–	0.52 ± 0.24
[Ca/H]	0.10 ± 0.20	0.21 ± 0.17	0.15 ± 0.23	-0.02 ± 0.14	0.20 ± 0.16	0.27 ± 0.33
[Ti/H]	0.37 ± 0.23	0.40 ± 0.17	0.32 ± 0.26	0.27 ± 0.22	0.42 ± 0.20	0.59 ± 0.31
[Cr/H]	–	–	–	–	0.31 ± 0.19	–
[Fe/H]	0.14 ± 0.20	0.23 ± 0.10	0.18 ± 0.17	-0.11 ± 0.10	0.23 ± 0.09	0.27 ± 0.19
[Ni/H]	0.27 ± 0.10	0.35 ± 0.10	0.30 ± 0.21	0.00 ± 0.21	0.21 ± 0.19	0.52 ± 0.27

References: V404 Cygni: González Hernández et al. (2011); Centaurus X-4: González Hernández et al. (2005)A0620-00: González Hernández et al. (2004) Nova Scorpii 1994: González Hernández et al. (2008a); XTE J1118 + 480: González Hernández et al. (2008b); Cyg X-2: Casares et al. (2010) and Suárez-Andrés et al. (2015)

[a]The uncertainties on the stellar abundances given in this table have been derived without taking into account the error on the microturbulence

[b]Oxygen abundances are given in NLTE

exploded with a mass cut in the range 11–12.5 $M_\odot$, such that no significant amount of iron could escape from the collapse of the inner layers. It is very important to study abundances of O, Si, Mg, S, and C to confirm this scenario.

4.3.3 Cen X-4

Abundances of Fe, Ca, Ti, Ni, and Al have been obtained using VLT/UVES spectra (González Hernández et al. 2005). These elements are found to have super solar abundances. Iron is enhanced too with [Fe/ H] = 0. 23 ± 0. 10). Interestingly, Ti and Ni are moderately enhanced as compared with the average values of stars of similar iron content. These element abundances can be explained if the secondary star captured a significant amount of matter ejected from a spherically symmetric supernova explosion of a 4 $M_\odot$ He core progenitor and assuming solar abundances

as primordial abundances in the secondary star. The kinematic properties of the system indicate that the neutron star received a natal kick velocity through an aspherical supernova and/or an asymmetric neutrino emission. The former scenario might be ruled out since the model computations cannot produce acceptable fits to the observed abundances.

4.3.4 V4641 Sgr

Spectroscopic analysis of this system has been carried out by Orosz et al. (2001). Peculiar abundance patterns have been claimed from the analysis of low- and high-resolution spectra obtained with different instruments. These authors found that N and Ti are enhanced about ten times compared to the Sun, Mg overabundance is about five to seven times, and O is three times the solar value, while Si is about solar. Given the physical characteristics of the companion star (mass, rotation, evolutionary stage), it is impossible to understand how and why Ti is extremely enhanced, while Si is solar. More spectral lines, better analysis, and better quality spectra are needed to confirm and expand this study. Given the effective temperature of the star, NLTE studies are mandatory.

4.3.5 XTE J1118 + 480

Abundances of Mg, Al, Ca, Fe, Ni, Si, and Ti have been derived using medium-resolution optical spectra of the secondary star in the high Galactic latitude black hole X-ray binary XTE J1118 + 480 (González Hernández et al. 2006). The super solar abundances indicate that the black hole in this system formed in a supernova event, whose nucleosynthetic products could pollute the atmosphere of the secondary star, providing clues on the possible formation region of the system, either Galactic halo, thick disk, or thin disk. A grid of explosion models with different He core masses, metallicities, and geometries has been explored. Metal-poor models associated with a formation scenario in the Galactic halo provide unacceptable fits to the observed abundances, therefore rejecting a halo origin for this X-ray binary. The thick-disk scenario produces better fits, although they require substantial fallback and very efficient mixing processes between the inner layers of the explosion and the ejecta. This makes very unlikely that the system was born in the thick disk. The best agreement between the model predictions and the observed abundances is obtained for metal-rich progenitor models. In particular, nonspherically symmetric models are able to explain, without strong assumptions of extensive fallback and mixing, the observed abundances. Moreover, asymmetric mass ejection in a supernova explosion could account for the required impulse necessary to eject the system from its formation region in the Galactic thin disk to its current halo orbit.

4.3.6 V404 Cyg

The atmospheric abundances of O, Na, Si, Ti, Mg, Al, Ca, Fe, and Ni have been derived using KeckI/HIRES spectra (González Hernández et al. 2011). The abundances of Si, Al, and Ti are slightly enhanced when comparing with average values in thin-disk solar-type stars. The O abundance, derived from optical lines,

is clearly enhanced in the atmosphere of the secondary star in V404 Cygni. This, together with the peculiar velocity of this system as compaed with the Galactic velocity dispersion of thin-disk stars, suggests that the black hole formed in a supernova or hypernova explosion. Different supernova/hypernova models having various geometries to study possible contamination of nucleosynthetic products in the chemical abundance pattern of the secondary star have been explored (e.g. Nakamura et al. 2001). A reasonable agreement between the observed abundances and the model predictions has been found (González Hernández et al. 2011). However, the O abundance seems to be too high regardless of the choice of explosion energy or mass cut, when trying to fit other element abundances. Moreover, Mg appears to be underabundant for all explosion models, which produces Mg abundances roughly two times higher than the observed value. The case of V404 Cyg is very peculiar and more studies are required to understand these observations.

4.3.7 Cyg X-2

Suárez-Andrés et al. (2015) have investigated abundances of O, Mg, Si, Ca, S, Ti, Fe, and Ni. The system is metal rich ([Fe/H] = 0, 27±0,19), and abundances of some alpha-elements (Mg, Si, S, Ti) are enhanced (see Fig. 8). This is consistent with a scenario of contamination of the secondary star during the supernova event. Strange enough, oxygen appears to be underabundant, whereas Fe and Ni are enhanced.

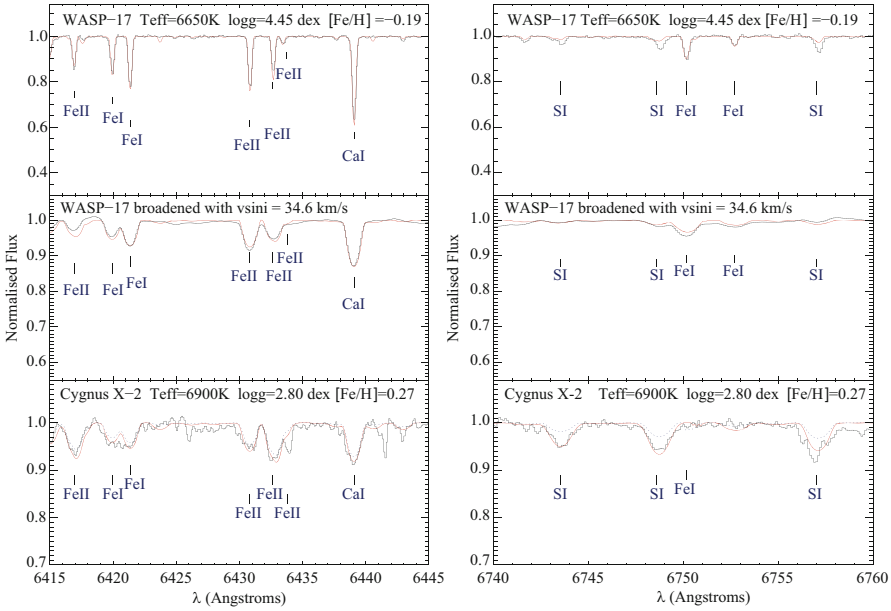

Fig. 8 Best synthetic fit to the UES spectrum of the secondary star in the neutron star X-ray binary Cygnus X-2 (*bottom panel*) and best fit to our template, with and without rotational broadening (*middle* and *top panels*). Synthetic spectra are computed for best-fit abundances (*solid line*) and for solar abundances (*dashed line*) (Figures taken from Suárez-Andrés et al. 2015)

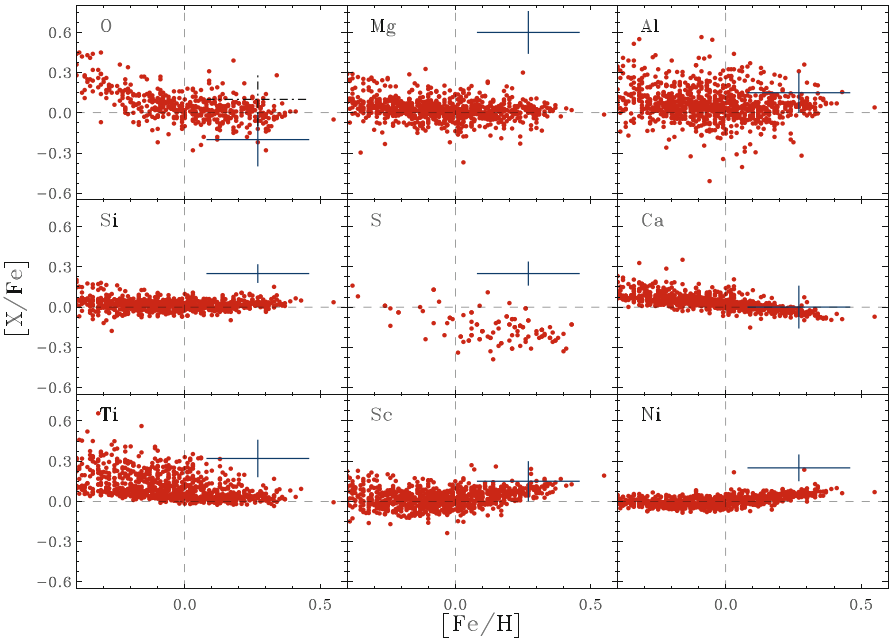

Fig. 9 Abundance ratios of the secondary star in Cyg X-2 (wide cross with errors) in comparison with the abundances of solar-type metal-rich dwarf stars (Taken from Suárez-Andrés et al. 2015)

Assuming that these abundances come from the matter that has been processed in the supernova and then captured by the secondary star, Suárez-Andrés et al. (2015) explored different supernova explosion scenarios with diverse geometries. A nonspherically symmetric supernova explosion, with a low mass cut, seems to reproduce better the observed abundance pattern of the secondary star compared to the spherical case. These authors have searched for anomalies in the abundance pattern of the secondary star by comparing their results with Galactic trends (see Fig. 9 taken from Suárez-Andrés et al. (2015) and reference from that article).

As it is shown in Fig. 9, most of the elements in Cygnus X-2 show overabundances when compared with Galactic trends, with the exception aluminum, calcium, and cadmium, which are consistent with those trends.

5 Cross-References

▸ Supernovae and the Evolution of Close Binary Systems
▸ The Masses of Neutron Stars

Acknowledgements JC would like to thank the hospitality of the Department of Physics of the University of Oxford, where this work was performed during a sabbatical visit. He also thanks Phil Charles for useful comments and discussions. Finally, JC acknowledges support by DGI of the

Spanish Ministerio de Educación, Cultura y Deporte under grants AYA2013-42627 and PR2015-00397, and from the Leverhulme Trust Visiting Professorship Grant VP2-2015-046. GI thanks Lucía Suárez and Jonay González Hernández for useful discussions. PGJ would like to thank James Miller–Jones for many useful discussions and his approval to use data on GX 339−4 and Swift J1753.0−0127 before their final publication. PGJ acknowledges funding from the European Research Council under ERC Consolidator Grant Agreement No. 647208.

References

Alpar MA, Cheng AF, Ruderman MA, Shaham J (1982) A new class of radio pulsars. Nature 300:728–730

Belczynski K, Wiktorowicz G, Fryer CL, Holtz DE, Kalogera V (2012) Missing black holes unveil the supernova explosion mechanism. ApJ 757:91–96

Blaauw A (1961) On the origin of the O- and B-type stars with high velocities (the "run-away" stars), and some related problems. Bull Astron Inst Neth 15:265–290

Brown GE, Heger A, Langer N, Lee C-H, Wellstein S, Bethe HA (2001) Formation of high mass X-ray black hole binaries. New Astron 6:457–470

Cantrell AG, Bailyn CD, McClintock JE, Orosz JA (2008) Optical state changes in the X-ray-quiescent black hole A0620-00. ApJL 673:L159–L162

Casares J, González Hernández JI, Israelian G, Rebolo R (2010) On the mass of the neutron star in Cyg X-2. MNRAS 401:2517–2520

Casares J, Negueruela I, Ribó M, Ribas I, Paredes JM, Herrero A, Simón-Díaz S (2014) A Be-type star with a black-hole companion. Nature 505:378–381

Casares J, Jonker PG (2014) Mass Measurements of Stellar and Intermediate-Mass Black Holes. Space Sci Rev 183:223–252

Charles PA, Coe MJ (2006) Optical, ultraviolet and infrared observations of X-ray binaries. In: Lewin W, van der Klis M (eds) Compact stellar X-ray sources. Cambridge astrophysics series, vol 39. Cambridge University Press, Cambridge, pp 215–265

Chomiuk L, Strader J, Maccarone TJ, Miller-Jones JCA, Heinke C, Noyola E et al (2013) A radio-selected black hole X-ray binary candidate in the milky way globular cluster M62. ApJ 777: 69–77

Clark JS, Goodwin SP, Crowther PA, Kaper L, Fairbairn M, Langer N et al (2002) Physical parameters of the high-mass X-ray binary 4U1700-37. A&A 392:909–920

Collins GW II, Sonneborn GH (1977) Some effects of rotation on the spectra of upper-main-sequence stars. ApJ Suppl 34:41–94

Dehnen W, Binney JJ (1998) Local stellar kinematics from HIPPARCOS data. MNRAS 298: 387–394

Dhawan V, Mirabel IF, Ribó M, Rodrigues I (2007) Kinematics of Black Hole X-Ray Binary GRS 1915+105. ApJ 668:430–434

Farr WM, Sravan N, Cantrell A, Kreidberg L, Bailyn CD, Mandel I, Kalogera V (2011) The mass distribution of stellar-mass black holes. ApJ 741:103–121

Fryer CL, Kalogera V (2001) Theoretical black hole mass distributions. ApJ 554:548–560

Gerke JR, Kochanek CS, Stanek KZ (2015) The search for failed supernovae with the large binocular telescope: first candidates. MNRAS 450:3289–3305

González ME, Stairs IH, Ferdman RD, Freire PCC, Nice DJ, Demorest PB et al (2011) High-precision timing of five millisecond pulsars: space velocities, binary evolution, and equivalence principles. ApJ 743:102–113

González Hernández JI, Rebolo R, Israelian G, Casares J, Maeder A, Meynet G (2004) Chemical abundances in the secondary star in the black Hole binary A0620-00. ApJ 609:988–998

González Hernández JI, Rebolo R, Israelian G, Casares J, Maeda K, Bonifacio P et al (2005) Chemical abundances in the secondary star of the neutron star binary centaurus X-4. ApJ 630:495–505

González Hernández JI, Rebolo R, Israelian G, Harlaftis ET, Filippenko AV, Chornock R (2006) XTE J1118+480: A Metal-rich Black Hole Binary in the Galactic Halo. ApJL 644: L49–L52

González Hernández JI, Rebolo R, Israelian G (2008a) The black hole binary nova Scorpii 1994 (GRO J1655–40): an improved chemical analysis. A&A 478:203–217

González Hernández JI, Rebolo R, Israelian G, Filippenko AV, Chornock R, Tominaga N et al (2008b) Chemical Abundances of the Secondary Star in the Black Hole X-Ray Binary XTE J1118+480. ApJ 679:732–745

González Hernández JI, Casares J, Rebolo R, Israelian G, Filippenko AV, Chornock R (2011) Chemical abundances of the secondary star in the black hole X-ray binary V404 Cygni. ApJ 738:95–107

Gualandris A, Colpi M, Portegies Zwart S, Possenti A (2005) Has the black hole in XTE J1118+480 experienced an asymmetric natal kick? ApJ 618:845–851

Honma M, Nagayama T, Ando K, Bushimata T, Choi YK, Handa T et al (2012) Fundamental Parameters of the Milky Way Galaxy Based on VLBI astrometry. PASJ 64:136

Hynes RI, Steeghs D, Casares J, Charles PA, O'Brien K (2004) The Distance and Interstellar Sight Line to GX 339-4. ApJ 609:317–324

Israelian G, Rebolo R, Basri G, Casares J, Martín EL (1999) Evidence of a supernova origin for the black hole in the system GRO J1655 – 40. Nature 401:142–144

Janka H-T (2013) Natal kicks of stellar mass black holes by asymmetric mass ejection in fallback supernovae. MNRAS 434:1355–1361

Johnson DRH, Soderblom DR (1987) Calculating galactic space velocities and their uncertainties, with an application to the ursa major group. AJ 93:864–867

Jonker PG, Nelemans G (2004) The distances to Galactic low-mass X-ray binaries: consequences for black hole luminosities and kicks. MNRAS 354:355–366

Joss PC, Rappaport SA (1984) Neutron stars in binary systems. Ann Rev Astron Astrophys 22:537–592

Knigge C, Coe MJ, Podsiadlowski P (2011) Two populations of X-ray pulsars produced by two types of supernova. Nature 479:372–375

Kochanek CS (2014) Failed supernovae explain the compact remnant mass function. ApJ 785:28–33

Kreidberg L, Bailyn CD, Farr WM, Kalogera V (2012) Mass measurements of black holes in X-ray transients: is there a mass gap? ApJ 757:36–52

Kurucz R (1993) ATLAS9 stellar atmosphere programs and 2 km/s grid. Kurucz CD-ROM, vol 13. Smithsonian Astrophysical Observatory, Cambridge, p 13

Lovegrove E, Woosley SE (2013) Very low energy supernovae from neutrino mass loss. ApJ 769:109–116

Lyne AG, Lorimer DR (1994) High birth velocities of radio pulsars. Nature 369:127–129

Maccarone TJ, Kundu A, Zepf SE, Piro AL, Bildsten L (2005) The discovery of X-ray binaries in the Sculptor dwarf spheroidal galaxy. MNRAS 364:L61–L65

Macdonald TD, Bailyn CD, Buxton M, Cantrell AG, Chatterjee R, Kennedy-Shaffer R et al (2014) The black hole binary V4641 sagitarii: activity in quiescence and improved mass determinations. ApJ 784:2–20

Mason AB, Norton AJ, Clark JS, Negueruela I, Roche P (2011) Preliminary determinations of the masses of the neutron star and mass donor in the high mass X-ray binary system EXO 1722-363. A&A 509:79–82

Mason AB, Norton AJ, Clark JS, Negueruela I, Roche P (2011) The masses of the neutron and donor star in the high-mass X-ray binary IGR J18027-2016. A&A 532:124–128

Mason AB, Clark JS, Norton AJ, Crowther PA, Tauris TM, Langer N et al (2012) The evolution and masses of the neutron star and donor star in the high mass X-ray binary OAO 1657-415. MNRAS 422:199–206

Mata Sánchez D, Muñoz-Darias T, Casares J, Steeghs D, Ramos Almeida C, Acosta Pulido JA (2015) Mass constraints to Sco X-1 from Bowen fluorescence and deep near-infrared spectroscopy. MNRAS 449:L1–L5

Miller-Jones JCA, Jonker PG, Nelemans G, Portegies Zwart S, Dhawan V, Brisken W et al (2009) The formation of the black hole in the X-ray binary system V404 Cyg. MNRAS 394: 1440–1448
Miller-Jones JCA, Jonker PG, Dhawan V, Brisken W, Rupen MP, Nelemans G et al (2009) The first accurate parallax distance to a black hole. ApJL 706:L230–L234
Miller-Jones JCA, Jonker PG, Maccarone TJ, Nelemans G, Calvelo DE (2011) A deep radio survey of hard state and quiescent black hole X-ray binaries. ApJL 739:L18–L23
Miller-Jones JCA (2014) Astrometric observations of X-ray binaries using very long baseline interferometry. PASA – Publ Astron Soc Aust 31:16–29
Mirabel IF, Dhawan V, Mignani RP, Rodrigues I, Guglielmetti F (2001) A high-velocity black hole on a Galactic-halo orbit in the solar neighbourhood. Nature 413:139–141
Mirabel IF, Mignani R, Rodrigues I, Combi JA, Rodriguez LF, Guglielmetti F (2002) The runaway black hole GRO J1655-40. A&A 395:595–599
Mirabel IF, Rodrigues I (2003) Formation of a black hole in the dark. Science 300:1119–1121
Muñoz-Darias T, Casares J, Martínez-Pais IG (2005) The "K-Correction" for Irradiated Emission Lines in LMXBs: Evidence for a Massive Neutron Star in X1822-371 (V691 CrA). ApJ 635:502–507
Muñoz-Darias T, Casares J, Martíinez-Pais IG (2008) The mass of the X-ray pulsar in X1822-371. In: 40 years of pulsaRS: millisecond pulsars, magnetars and more. AIP Conference Proceedings 983:542–544
Nakamura T, Umeda H, Iwamoto K, Nomoto K, Hashimoto M, Hix WR et al (2001) Explosive Nucleosynthesis in Hypernovae. ApJ 555:880–899
Nelemans G, Tauris TM, van den Heuvel EPJ (1999) Constraints on mass ejection in black hole formation derived from black hole X-ray binaries. A&A 352:L87–L90
O'Connor E, Ott CD (2011) Black Hole Formation in Failing Core-Collapse Supernovae. ApJ 730:70–89
Orosz J, Kuulkers E, van der Klis M, McClintock JE, Garcia MR, Callanan PJ et al (2001) A Black Hole in the Superluminal Source SAX J1819.3-2525 (V4641 Sgr). ApJ 555:489–503
Orosz JA, Steiner JF, McClintock JE, Buxton MM, Bailyn CD, Steeghs D et al (2014) The Mass of the Black Hole in LMC X-3. ApJ 794:154–171
Özel F, Psaltis D, Narayan R, McClintock JE (2010) The Black Hole Mass Distribution in the Galaxy. ApJ 725:1918–1927
Özel F, Psaltis D, Narayan R, Santos Villarreal A (2012) On the Mass Distribution and Birth Masses of Neutron Stars. ApJ 757:55–67
Piro AL (2013) Taking the "Un" out of "Unnovae". ApJL 768:L14–L18
Quaintrell H, Norton AJ, Ash TDC, Roche P, Willems B, Bedding TR et al (2003) The mass of the neutron star in Vela X-1 and tidally induced non-radial oscillations. A&A 401:313–323
Rawls ML, Orosz JA, McClintock JE, Torres MAP, Bailyn CD, Buxton MM (2011) Refined neutron star mass determinations for six eclipsing X-ray pulsar binaries. ApJ 730:25–35
Reid MJ, McClintock JE, Narayan R, Gou L, Remillard RA, Orosz JA (2011) The Trigonometric Parallax of Cygnus X-1. ApJ 742:83–87
Reid MJ, McClintock JE, Steiner JF, Steeghs D, Remillard RA, Dhawan V et al (2014) A Parallax Distance to the Microquasar GRS 1915+105 and a Revised Estimate of its Black Hole Mass. ApJ 796:2–9
Reig P (2011) Be/X-ray binaries. Astrophys Space Sci 332:1–29
Repetto S, Nelemans G (2015) Constraining the formation of black holes in short-period black hole low-mass X-ray binaries. MNRAS 453:3341–3355
Reynolds AP, Quaintrell H, Still MD, Roche P, Chakrabarty D, Levine SE (1997) A new mass estimate for Hercules X-1. MNRAS 288:43–52
Reynolds TM, Fraser M, Gilmore G (2015) Gone without a bang: an archival HST survey for disappearing massive stars. MNRAS 453:2885–2900
Russell TD, Miller-Jones JCA, Curran PA, Soria R, Altamirano D, Corbel S et al (2015) Radio monitoring of the hard state jets in the 2011 outburst of MAXI J1836-194. MNRAS 450: 1745–1759

Shahbaz T, Watson CA, Dhillon VS (2014) The spotty donor star in the X-ray transient Cen X-4. MNRAS 440:504–513
Shajn G, Struve O (1929) On the rotation of the stars. MNRAS 89:222–239
Smartt SJ, Eldridge JJ, Crockett RM, Maund JR (2009) The death of massive stars - I. Observational constraints on the progenitors of Type II-P supernovae. MNRAS 395:1409–1437
Smartt SJ (2015) Observational constraints on the progenitors of core-collapse supernovae: the case for missing high-mass star. PASA – Publ Astron Soc Aust 32:16–37
Steeghs D, Casares J (2002) The mass donor of scorpius X-1 revealed. ApJ 568:273–278
Strader J, Chomiuk L, Maccarone TJ, Miller-Jones JCA, Seth AC (2012) Two stellar-mass black holes in the globular cluster M22. Nature 490:71–73
Suárez-Andrés L, González Hernández JI, Israelian G, Casares J, Rebolo R (2015) Chemical abundances of the secondary star in the neutron star X-ray binary Cygnus X-2. MNRAS 447:2261–2273
Tomsick JA, Heindl WA, Chakrabarty D, Kaaret P (2002) Rotational Broadening Measurement for the Neutron Star X-Ray Transient XTE J2123-058. ApJ 581:570–576
Ugliano M, Janka H-T, Marek A, Arcones A (2012) Progenitor-explosion connection and remnant birth masses for neutrino-driven supernovae of iron-core progenitors. ApJ 757:69–78
van Paradijs J, White N (1995) The Galactic Distribution of Low-Mass X-Ray Binaries. ApJL 447:L33–L36
van Paradijs J (1998) Neutron stars and black holes in X-ray binaries. In: Buccheri R, van Paradijs J, Alpar MA (eds) The Many Faces of Neutron Stars, vol 515. Kluwer Academic Publishers, ASIC, Dordrecht/Boston, p 279
Wade RA, Horne K (1988) The radial velocity curve and peculiar TiO distribution of the red secondary star in Z Chamaeleontis. ApJ 324:411–430
Wang L, Steeghs D, Casares J, Charles PA, Muñoz-Darias T, Marsh TR et al (2017, in press) System mass constraints for the accreting millisecond pulsar XTE J1814-338 using Bowen fluorescence. MNRAS, arXiv:1612.06430
Wielen R (1977) The diffusion of stellar orbits derived from the observed age-dependence of the velocity dispersion. A&A 60:263–275
Wijnands R, van der Klis M (1998) A millisecond pulsar in an X-ray binary system. Nature 394:344–346
Willems B, Henninger M, Levin T, Ivanova N, Kalogera V, McGhee K et al (2005) Understanding compact object formation and natal kicks. I. Calculation methods and the case of GRO J1655-40. ApJ 625:324–346
Witte MG, Savonije GJ (2001) Tidal evolution of eccentric orbits in massive binary systems. II. Coupled resonance locking for two rotating main sequence stars. A&A 366:840–857
Wu J, Orosz JA, McClintock JE, Hasan I, BaiIyn CD, Gou L et al (2016) The mass of the black hole in the X-ray binary nova muscae 1991. ApJ 825:46–58
Zhang CM, Wang J, Zhao YH, Yin HX, Song LM, Menezes DP et al (2011) Study of measured pulsar masses and their possible conclusions. A&A 527:A83–A90
Zhang Z, Gilfanov M, Bogdán Á (2013) Low-mass X-ray binary populations in galaxy outskirts: globular clusters and supernova kicks. A&A 556:A9–A18